Temperature Dependence of Oxygen Diffusion into Clay-Doped PS Films

Şaziye Uğur,[1] Önder Yargı,[1] Önder Pekcan[2]
[1]*Department of Physics, Istanbul Technical University, 34469 Maslak, Istanbul, Turkey*

[2]*Faculty of Arts and Science, Kadir Has University, Cibali 34230, Istanbul, Turkey*

Fluorescence technique was employed for the measurement of the diffusion coefficient of oxygen into polystyrene (PS) latex/modified Na-activated bentonite (MNaLB) clay composite films. Three different MNaLB content (0, 5, and 20 wt%) composite films were prepared from PS/MNaLB mixtures by annealing them at 200°C, above the glass transition temperature of PS for 10 min. To determine the diffusivity of oxygen in PS/MNaLB composite films, diffusion measurements were performed over the temperature range from 25 to 70°C. Pyrene (P) was used as the fluorescent agent. The diffusion coefficients (*D*) of oxygen were determined by combining the fluorescence quenching method with Fickian transport model, and were found as a function of temperature for each MNaLB content film. The results showed that *D* values are strongly dependent on both temperature and clay content in composite film. It was also observed that *D* coefficients obey Arrhenius behavior, from where diffusion activation energies were measured. POLYM. COMPOS., 31:77–82, 2010. © 2009 Society of Plastics Engineers

INTRODUCTION

In the last few years, the use of polymers as coating materials for the protection of the active ingredient of solid pharmaceutical products against decomposition due to environmental conditions has been greatly increased. Apart from acting as a moisture barrier or controlling the release of the active agent, the most desirable property of these polymer films is their resistance to the gas diffusion. Because single component polymer films have poor mechanical and gas barrier properties, there has been growing interest in producing new materials by filling polymers with inorganic natural (minerals) and/or synthetic (carbon black and silica) compounds [1–5]. Typically, inorganic fillers like talc, mica, chalk, smectite, and bentonite are used in these new materials. In recent years, polymer/clay (P/C) nanocomposites have become increasingly important because they combine the structural, physical, and chemical properties of both clay and polymer [6, 7]. The efficiency of clay modifies many different properties of the polymer, such as sorbancy, ion exchange capabilities, and thermal and solvent resistance. They give improved mechanical properties, gas barrier properties, and decreased flammability relative to the simple polymers [8].

The enhancement in barrier properties in composites depends on several factors, such as the amount, length, and width of the filler, orientation and dispersion of the filler particles. For more than 50 years, polymer scientists have been interested in the influence of fillers on gas diffusion through polymer membrane [9–12]. This analysis provides us important knowledge about the effect of mineral fillers on the performance of oxygen sensors. Gorrasi et al. [10] studied the transport properties of *n*-pentane and dichloromethane vapors in polypropylene-organophilic layered silicates nanocomposites with different clay concentrations. It was found that the permeability of both solvent vapors was reduced, mainly due to the decreased diffusion, because the solubility was less affected by the presence of fillers. Lu et al. [11] examined the influence of 10-nm diameter silica particles on oxygen diffusion in PDMS polymer film. A decrease was observed in oxygen diffusion coefficients, D with increasing silica content. This reduction in D was attributed to the tortuous path toward diffusing gas molecules and reduced molecular mobility of polymer chains caused by the filler particles. Bharadwaj [12] also addressed the modeling of gas barrier properties in polymer-layered silicate nanocomposites based on a tortuosity argument. It was considered that the presence of filler introduces a tortuous path for a diffusing penetrant. The reduction of permeability arises from the longer diffusive path that the penetrants must travel in the presence of the layered silicate.

The usual procedure used to measure the diffusion coefficients of gases through polymeric system are based

Correspondence to: Şaziye Uğur; e-mail: saziye@itu.edu.tr
DOI 10.1002/pc.20768
Published online in Wiley InterScience (www.interscience.wiley.com).
© 2009 Society of Plastics Engineers

upon measurements of the amount of gas which permeates a given area of polymer in a given time. In addition to this direct method of determination, depending upon the properties of the gases being investigated there are also indirect methods based on the quenching or bleaching action of these gases on the molecular probes imbedded uniformly in the polymer. Several spectroscopic techniques that utilize oxygen quenching to determine the rate of oxygen diffusion through polymer films have been reported [13–15]. Guillet obtained values of diffusion coefficients of oxygen in different polymer matrix by luminescent quenching experiments [14]. Fluorescence method has also been used for monitoring diffusion of small molecules in polymer films [14, 15]. The diffusion coefficient of oxygen into poly(methyl methacrylate) (PMMA) was determined by the quenching of phosphorescence of phenanthrene added into polymer [16]. Barker has utilized the bleaching action of oxygen on color centers produced by electron beam irradiation of polycarbonate and PMMA by following optically the moving boundary [17]. The quenching of fluorescence of naphthalene in PMMA was studied by oxygen in thin films after displacement of nitrogen atmosphere over the sample by oxygen [18]. In some of our earlier studies, we examined the effects of annealing and packing on the oxygen diffusion coefficient, D, in PMMA [19, 20] by using steady state fluorescence (SSF) and photon transmission (PT) techniques. Values of D were recorded depending on the film thickness and annealing temperature for polymer samples exposed to ambient oxygen atmospheres. It was found that while the D values increased by increasing the film thickness [19], no temperature effect [20] was observed on the diffusion coefficient, D.

The present study involves the diffusion behavior of oxygen in PS/MNaLB composite films depending on temperature with varying MNaLB contents. Three different sets of composite films were prepared from pyrene labeled PS latex and MNaLB clay mixtures with 0, 5, and 20 wt% MNaLB content by annealing at 200°C for 10 min. SSF technique was used to study oxygen diffusion into these films over the temperature range of 25–70°C. The time drive mode of SSF spectrometer was employed to monitor the intensity change of excited pyrene (P) during oxygen penetration into composite films. A model was developed for low quenching efficiency to measure oxygen diffusion coefficient, D.

EXPERIMENTAL

MNaLB Clay

The Na-activated bentonite (NaLB) was obtained from natural bentonite, which was collected from the bentonite deposits in Lalapaşa-Edirne, Thrace, Turkey (courtesy of Bensan) (35% humidity) by treating the clay with 4% (w/w) $NaHCO_3$ solution. NaLB was dispersed in distillated water at room temperature mixing for 24 h (6 wt.% NaLB stock dispersion). Meanwhile, the natural pH value of NaLB was found to be 10.7. Benzyldimethyltetradecyl ammonium chloride (BDTDACl) cationic surfactant was dissolved in water at 20 mmol/l concentration. Then 5 ml BDTDACl stock solution, 6.25 ml 6 wt.% NaLB stock dispersion, and 1.25 ml distillated water were mixed, and the dispersion was shaken in order to obtain 3 wt.% NaLB + 8 mmol/l BDTDACl (modified clay). This dispersion was shaken overnight and an adsorption time of 24 h was adopted for surfactant. As a result, modified clay (MNaLB) dispersion was obtained and diluted to contain 0.0141g/ml MNaLB. The particle size distributions (PSDs) of bentonitic clays were determined by the sedimentation technique and was measured to be in the range of 50–0.4 μm, and average particle size of NaLB was 10 μm. After the modification of clay, the PSD of MNaLB was measured to be in the range of 10–0.4 μm, and average particle size of sample was 1 μm. In original NaLB dispersion, coarser than 10 μm fractions are 49.8%, but no clay particle above 10 μm was found after the addition of BDTDACl [21]. On the other hand, although the particle size was decreasing, the surface area of particles increased. As a result, MNaLB contains much smaller clay particles due to their strong dispersion performance [22].

PS Latex

Pyrene labeled polystyrene particles were produced via emulsifier-free radical polymerization process. The polymerization reaction was carried out under emulsifier-free radical polymerization conditions in a 200 ml thermostated round-bottomed four-necked flask, equipped with a glass anchor-shaped stirrer, condenser and nitrogen inlet. Styrene monomer was first introduced in the reactor containing boiled and deionized water and the fluorescent monomer 1-pyrenylmethyl methacrylate (PolyFluor^{TM}394) was first dissolved in small amount of styrene. The potassium persulfate (KPS) initiator was dissolved in water and added when the polymerization temperature was equilibrated at 70°C. The stirring rate was adjusted to 300 rpm. The recipe of the prepared latex is summarized as follows: 100 ml water, 4 g of styrene, 0.1 g of KPS (dissolved in 2 ml water), and 0.0129 g of fluorescent monomer (dissolved in 1 g styrene). The polymerization reaction was conducted during 18 h under nitrogen condition. The particles are spherical and fairly monodisperse, having all very similar mean diameters (320 nm).

Film Preparation

PS/MNaLB composite films were prepared by the casting method. Distilled water was used to disperse the used materials. Three different films with 0, 5, and 20 wt% MNaLB content were prepared from the dispersion

 DOI 10.1002/pc

of PS latex/MNaLB clay. Dry films were obtained by placing the same number of drops on a glass plates with the size of 0.8 × 2.5 cm^2 and allowing the water to evaporate. Film samples then were annealed at 200°C, above T_g of PS (=105°C) for 10 min. Before fluorescence measurements were performed. Film thicknesses were measured and found to be around 13 μm.

Films were placed in a quartz cell filled with nitrogen, and fluorescence measurements were performed for oxygen diffusion experiments, in Perkin Elmer Model LS-50 fluorescence spectrophotometer. Slit widths were kept at 8 nm. Experiments were carried out at 25–70°C temperature range. A thermistor-based digital temperature probe in spectrophotometer chamber was used to monitor temperatures which were observed to remain constant within ±2°C during the course of diffusion measurements. In all experiments, P was excited at 345 nm and the emission maximum at 395 nm was used for fluorescence intensity measurements. P intensity, I was monitored against time by using time-drive mode of spectrophotometer at different temperatures for each clay content composite film, after the quartz tube was open to the air for O_2 diffusion experiments. Because the diffusion measurements required that oxygen permeate only one surface of the film, then to be ensured to eliminate the lateral diffusion of oxygen, the opposite side of the cell window was masked using black tape on.

THEORETICAL CONSIDERATIONS

Fluorescence Quenching by Oxygen

The mechanism of oxygen quenching involves a sequence of spin allowed internal conversion processes, which takes place within a weakly associated encounter complex between probe and oxygen. The product is either a singlet ground state or an excited triplet species [23].

Data generated from oxygen quenching studies on small molecules in homogeneous solution are usually analyzed using the Stern–Volmer relation (*Eq. 1*), provided that the oxygen concentration $[O_2]$ is not too high [24].

$$\frac{I_0}{I} = 1 + k_q \tau_0 [O_2]. \quad (1)$$

In this equation, I and I_0 are the fluorescence intensities in the presence and absence of oxygen, respectively, k_q is the bimolecular quenching rate constant and τ_0 is the fluorescence lifetime in the absence of O_2. This equation requires that the decay of fluorescence is single exponential and, moreover, that quenching interactions occur with a unique rate constant k_q. From the slope of a plot of I_0/I versus $[O_2]$, k_q can be determined provided that τ_0 is known.

Diffusion in Plane Sheet

Fick's second law of diffusion was used to model diffusion phenomena in plane sheet. The following equation is obtained by assuming a constant diffusion coefficient, for concentration changes in time [25]

$$\frac{C}{C_0} = \frac{x}{d} + \frac{2}{\pi}\sum_{n=1}^{\infty}\frac{\cos n\pi}{n}\sin\frac{n\pi x}{d}\exp\left(-\frac{Dn^2\pi^2 t}{d^2}\right) \quad (2)$$

where d is the thickness of the slab, D is the diffusion coefficient of the diffusant, and C_0 and C are the concentration of the diffusant at time zero and t, respectively. x corresponds to the distance at which C is measured. We can replace the concentration terms directly with the amount of diffusant, M by using the following relation:

$$M = \int_v C dV \quad (3)$$

when *Eq. 3* is considered for a volume element in the plane sheet and substituted in *Eq. 2*, the following solution is obtained [25]:

$$\frac{M_t}{M_\infty} = 1 - \frac{8}{\pi^2}\sum_{n=0}^{\infty}\frac{1}{(2n+1)^2}\exp\left(-\frac{D(2n+1)^2\pi^2 t}{d^2}\right) \quad (4)$$

where M_t and M_∞ represent the amounts of diffusant entering the plane sheet at time t and infinity, respectively.

RESULTS AND DISCUSSIONS

Oxygen Diffusion

Normalized pyrene intensity, I_t curves are presented in Fig. 1 as a function of time for the 5 wt% MNaLB content film exposed to oxygen at elevated temperatures. It is seen that as oxygen diffused through the planar film, the

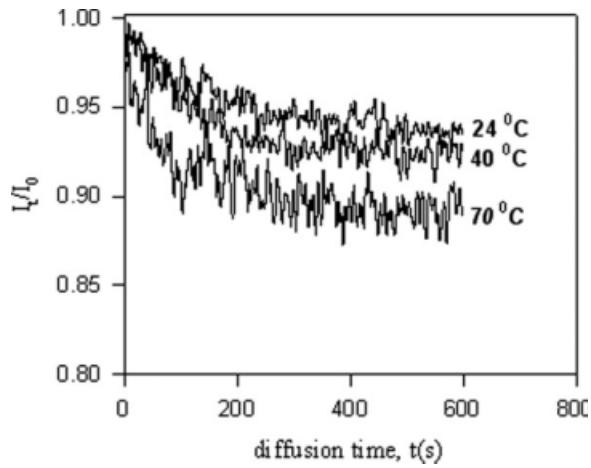

FIG. 1. The time behavior of the pyrene, P, fluorescence intensity, I, during oxygen diffusion into the 5 wt% MNaLB content film at various temperatures. Numbers on each curves indicate the temperature.

emission intensity of the pyrene decreased according to *Eq. 1* at each temperature. The rate of decrease in intensity was higher at high temperatures predicting that higher temperature allows more O_2 molecules diffused into the films, and as a result rapid quenching of excited pyrene molecules takes place. The curves reached their equilibrium value almost in the same fashion, as oxygen diffused through and equilibrated in the film. To interpret the above findings, *Eq. 1* can be used by expanding in a series for low quenching efficiency, i.e. $k_q\tau_0[O_2] \ll 1$ which then produces the following useful result

$$I \approx I_0\left(1 - k_q\tau_0[O_2]\right). \tag{5}$$

During diffusion into the films, excited P molecules are quenched in the volume which is occupied by O_2 molecules at time, t. Then P intensity at time t can be represented by the volume integration of *Eq. 5* as

$$I_t = \frac{\int I dv}{\int dv} = I_0 - \frac{k_q\tau_0 I_0}{V}\int dv[O_2] \tag{6}$$

where dv and V are the differential and total volume of the film as shown in Fig. 2. In Fig. 2, oxygen diffusion into the film is presented at different time steps, where pyrene quenching take place at $t > 0$ and levels off at $t = \infty$. Performing the integration, the following relation is obtained

$$I_t = I_0\left(1 - k_q\frac{\tau_0}{V}O_2(t)\right) \tag{7}$$

where $O_2(t) = \int dv[O_2]$ is the amount of oxygen molecules diffuse into the film at time t. Here, it can be assumed that $O_2(t)$ corresponds to M_t in *Eq. 4*. Combining *Eq. 4* for oxygen diffusion with *Eq. 7* the following relation is produced to interpret the diffusion curves in Fig. 1:

$$\frac{I_t}{I_0} = A + \frac{8C}{\pi^2}\exp\left(-\frac{D\pi^2 t}{d^2}\right) \tag{8}$$

where d is the film thickness, D is the diffusion coefficient of oxygen, $C = k_q\tau_0 O_2(\infty)/V$ and $A = 1 - C$. Here $O_2(\infty)$ is the amount of oxygen molecules diffuse into the film at time infinity. The logarithmic form of *Eq. 8* can be written as follows:

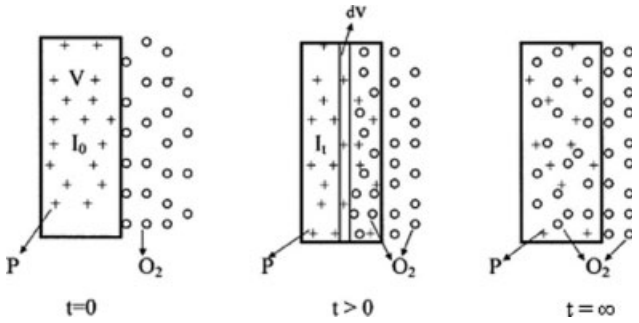

FIG. 2. Cartoon representation of oxygen diffusion into the film at elevated time intervals.

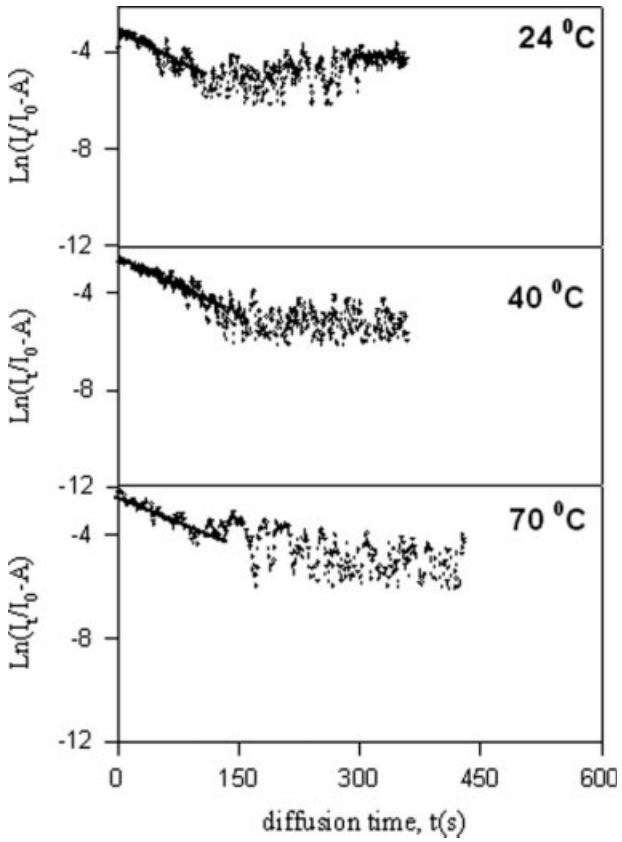

FIG. 3. Logarithmic plot of the data in Fig. 1 according to *Eq. 9* in the text. The slopes of the curves produced diffusion coefficients, D. Numbers on each curve show the temperatures.

$$\mathrm{Ln}\left(\frac{I_t}{I_0} - A\right) = \mathrm{Ln}\left(\frac{8C}{\pi^2}\right) - \frac{D\pi^2}{d^2}t. \tag{9}$$

Figure 3a–c presents $\mathrm{Ln}(I_t/I_0 - A)$ versus diffusion time for the 5 wt% MNaLB content film at various temperatures. *Equation 9* is fitted to these data by using the linear least square method and the oxygen diffusion coefficients, D at different temperatures were estimated from the slopes of the plots. Similar fittings were done for the oxygen diffusing into the other MNaLB content films. k_q and D values, obtained at different temperatures are collected in Table 1. The average k_q and D values were determined

TABLE 1. Experimentally obtained diffusion (D) and quenching rate constants (k_q) at various temperatures.

	$D \times 10^{-10}$ ($cm^2\ s^{-1}$)			$k_q \times 10^7$ ($M^{-1}\ s^{-1}$)		
T (°C)	0	5	20	0	5	20
24	7.3	21.0	27.7	3.8	3.0	4.9
40	7.4	20.4	27.9	3.3	5.4	6.3
50	9.4	24.4	27.7	4.5	3.6	7.3
60	11.4	24.8	28.2	5.0	6.8	5.7
70	12.0	25.7	28.5	5.2	5.4	5.7

DOI 10.1002/pc

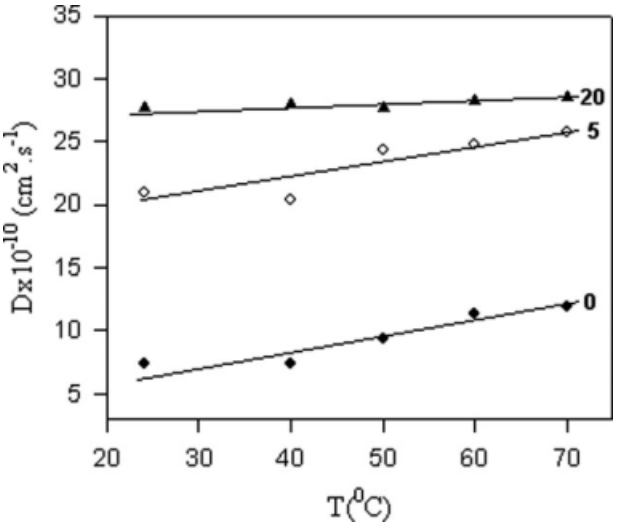

FIG. 4. Plot of the diffusion coefficients, D versus temperatures, T for the 0, 5, and 20 wt% MNaLB content films.

from 3 or 5 sequential measurements for different samples in each case. D values versus temperatures are plotted for three MNaLB content films in Fig. 4. It is seen that D coefficients are strongly dependent on both temperature and MNaLB fraction in the film. It is worthy to note that D values increase with increasing temperature for all composite films, as expected. However, the rate of increase in D values for 0 and 5 wt% MNaLB is found to be greater than that of 20 wt% MnaLB content film. Only a slight increase is seen in D values of 20 wt% MNaLB content film with respect to temperature. In addition, for a given temperature D values for 5 and 20 wt% MNaLB content films are ~2–4 times greater than that of pure PS film. These results suggest that increasing the clay content in the film screens the PS latex by preventing the interdiffusion of polymer chains to form a continuous film [26]. This behavior would suggest a rather bad adherence of clay particles to the polymer matrix, which results in the formation of defects or voids in the films that enhance the diffusion rate of oxygen along the film by increasing the surface area against oxygen molecules. From here one expects more rapid oxygen diffusion [20] into 5 and 20 wt% MNaLB content films due to presence of a large numbers of microvoids created in these films. The slight variation of D with respect to temperature in 20 wt% MNaLB content film can also be explained with the high porosity of this film, which presents a similar medium for oxygen diffusion at all temperatures.

It is known that the addition of a filler into polymer films above a critical percentage creates voids [27, 28] in the polymer matrix. Ponomarev and Gouterman [27] have reported that the addition of high amounts of titanium oxide (TiO_2) in PSP film cause the presence of a large fraction of microvoids inside the films. As a result, air can diffuse very rapidly to the inside of the coating through these voids. Kneas et al. [28] studied the effect of silica (S) on diffusion coefficients, D of oxygen for pTMSMMA films. They found a two-fold decrease in D with increasing amounts of silica. They explained this decrease as a result of the strong adsorption of oxygen onto the hydrophobic amorphous silica particles due to their large surface area which acts as a trap for oxygen molecules. Cox and Dunn [13, 29, 30] investigated the influence of temperature on diffusion of oxygen into silica filled silicone films by using fluorescence quenching method. Despite the increase in diffusion coefficients with temperature, they observed a decrease in D values with increasing silica content. They explained the decrease in D both by obstacle effects of filler and oxygen adsorption on its surface.

On the other hand, oxygen diffusion coefficients obtained in this study (10^{-10} cm^2 s^{-1}) is in the same order of magnitude with those previously obtained for PMMA films [20] of different thicknesses (10–100 μm) by using the same technique. Because of high packing of latex particles, thicker films contain cracks and pores which can cause faster diffusion of oxygen molecules into these films. However, D values for this study (10^{-10} cm^2 s^{-1}) is one order larger than that obtained for PMMA films (10^{-11} cm^2 s^{-1}) annealed at various temperatures [19]. Because the thickness of PMMA films (≈12 μm) is almost the same with the films used in this study, this difference can be originated from the absence of voids in PMMA films due to the formation of a mechanically strong, void-free continuous matrix during annealing, which hinders the diffusive processes from the film surface.

Diffusion Activation Energies

The transport of gases through the membranes can be described as thermally activated process that obeys the

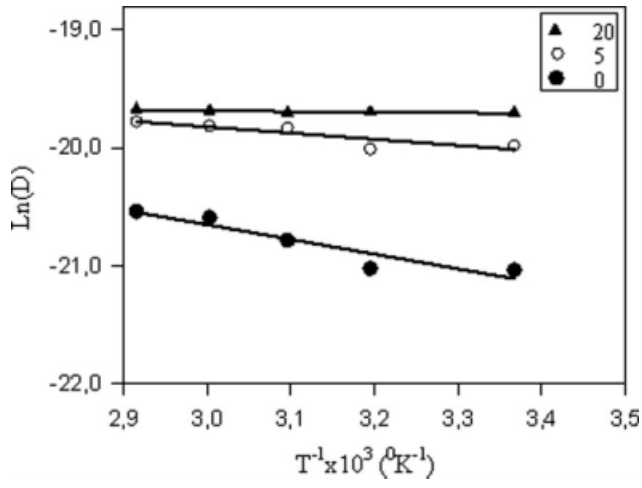

FIG. 5. Plot of the logarithmic form of *Eq. 10* for the data in Table 1. ΔE_D values are obtained from the slopes of the straight lines for each MNaLB content film, respectively.

TABLE 2. Experimentally produced activation energies (ΔE_D).

W_{MNaLB} (wt%)	0	5	20
ΔE_D (kJ mol^{-1})	10.2	4.3	0.5

Arrhenius behavior. The temperature dependence of D coefficient can be written as follows:

$$D = D_0 \exp\left(\frac{-\Delta E_D}{k_B T}\right) \quad (10)$$

Here k_B is the Boltzmann constant, D_0 is pre-exponential factor, ΔE_D is the activation energy as associated with the oxygen diffusion. The activation energy was determined from the logarithmic plots of the D coefficient against the reciprocal of the absolute temperature. In Fig. 5, Ln(D) is plotted versus 1000/T for the different clay fractions, respectively. The value of activation energy associated with oxygen diffusion (ΔE_D) for different clay fractions was calculated from the slope of these plots fitting the data in Fig. 5 to the *Eq. 10* by a least square fit. The results are given in Table 2 where ΔE_D decreases with increasing clay content, which confirms our above assumption. In other words, the energy need for the oxygen diffusing in the porous medium is much less than they do in rigid environment.

CONCLUSION

The diffusion of oxygen into PS-MNaLB composite films was studied at elevated temperatures for different clay contents by using fluorescence quenching method. The oxygen diffusion (D) coefficients and related activation energies in these composite films were determined and compared. The results showed that diffusion of oxygen was accelerated by both an increase in clay fraction and temperature. The high diffusion rate of oxygen in the composite is attributed to the formation of voids (pores) in the film which facilitates oxygen diffusion. The decrease in the activation energy associated with the oxygen diffusion process (ΔE_D) is observed with increase in clay fraction. In conclusion, this work has shown that simple SSF technique can be used to measure the diffusion coefficient of oxygen molecules into composite films quite accurately.

REFERENCES

1. R.A. Vara, K.D. Jandt, F.J. Kramer, and F.P. Giannelis, *Chem. Mater.*, **8**, 2628 (1996).
2. M.W. Noh and D.C. Lee, *Polym. Bull.*, **42**, 619 (1999).
3. H.Z. Friedlander and C.R. Grink, *J. Polym. Sci. Polym. Lett.*, **2**, 475 (1964).
4. C. Kato, K. Kuroda, and H. Takahara, *Clay Clay Miner.*, **29**, 294 (1981).
5. J.G. Doh and I. Cho, *Polym. Bull.*, **41**, 511 (1998).
6. Ş. Uğur, A. Alemdar, and Ö. Pekcan, *J. Coat. Tech. Res.*, **2**, 565 (2005).
7. Ş. Uğur, A. Alemdar, and Ö. Pekcan, *Polym. Compos.*, **27**, 299 (2006).
8. Y. Li, B. Zhao, S.B. Xie, and S. Zhang, *Polym. Int.*, **52**, 892 (2003).
9. R.M. Barrer, in *Diffusion in Polymers*, J. Crank and G.S. Park, Eds., Academic Press, New York, 164–217, (1968).
10. G. Gorrasi, M. Tortora, V. Vittoria, D. Kaempfer, and R. Mülhaupt, *Polymer* **44**, 3679 (2003).
11. X. Lu, I. Manners, and M.A. Winnik, *Macromolecules* **34**, 1917 (2001).
12. R.K. Bharadwaj, *Macromolecules* **34**, 9189 (2001).
13. M.E. Cox and B. Dunn, *Appl. Opt.*, **24**, 2114 (1985).
14. J.E. Guillet, in *Photophysical and Photochemical Tools in Polymer Science*, M.A. Winnik, Ed., Reidel, Dordrecht, The Netherlands, 467 (1986).
15. J.E. Guillet, *Polymer Photophysics and Photochemistry*, Cambridge University Press, Cambridge (1985).
16. G. Shaw, *Trans. Faraday Soc.*, **63**, 2181 (1967).
17. R.E. Barker, *J. Polym. Sci.*, **58**, 553 (1962).
18. J.R. MacCallum and A.L. Rudkin, *Eur. Polym. J.*, **14**, 655 (1978).
19. O. Pekcan and S. Ugur, *J. Coll. Interface Sci.*, **217**, 154 (1999).
20. O. Pekcan and S. Ugur, *Polymer* **41**, 7531 (2000).
21. E. Gunister, N. Gungor, and O.I. Ece, *Mater. Lett.*, **60**, 666 (2006).
22. E. Günister, C.H. Unlu, O. Atici, O.I. Ece, and N. Gungor, *J. Compos. Mater.*, **41**, 153 (2007).
23. J.B. Birks, *Organic Molecular Photophysics*, Wiley-Interscience, New York (1975).
24. S.A. Rice. "Diffusion-Limited Reactions," in *Comprehensive Chemical Kinetics*, C.H. Bamford, C.F.H. Tipper, and R.G. Compton, Eds., Elsevier, Amsterdam (1985).
25. J. Crank, *The Mathematics of Diffusion*, Oxford University Press, London (1970).
26. S. Ugur, O. Yargi, E. Gunister, and O. Pekcan, *Appl. Clay Sci.* (in press).
27. S. Ponomarev and M. Gouterman, in *The Sixth Annual Pressure Sensitive Paint Workshop*, Seattle, WA, October 6–8 (1998).
28. K.A. Kneas, J.N. Demas, B. Nguyen, A. Lockhart, W. Xu, and B.A. DeGraff, *Anal. Chem.*, **74**, 1111 (2002).
29. M.E. Cox and B. Dunn, *J. Polym. Soc. A: Polym. Chem.*, **24**, 621 (1986).
30. M.E. Cox and B. Dunn, *J. Polym. Sci. A: Polym. Chem.*, **24**, 2395 (1986).

 DOI 10.1002/pc